PCCP

Accepted Manuscript

ROYAL SOCIETY OF CHEMISTRY

www.rsc.org/pccp

PCCP

COMMUNICATION

Stable n-type doping of graphene via high-molecular-weight ethylene amines

Received 00th January 20xx,
Accepted 00th January 20xx

DOI: 10.1039/x0xx00000x

www.rsc.org/

Insu Jo,[a] Youngsoo Kim,[a,b] Joonhee Moon,[a] Subeom Park,[a] Jin San Moon,[c] Won Bae Park,[c] Jeong Soo Lee[c*] and Byung Hee Hong[a*]

We demonstrate a stable and strong n-type doping method to tune the electrical properties of graphene via vapor phase chemical doping with various high-molecular-weight ethylene amines. The resulting carrier concentration after doping with pentaethylenehexamine (PEHA) is as high as -1.01 x 10^{13} cm^{-2}, which reduces the sheet resistance of graphene up to ~400% compared to pristine graphene. Our study suggests that the branched structure of dopant molecules is an another important factor that determines the actual doping degree on graphene.

Graphene has been intensively studied owing to its unusual band structure and electrical tunability that are particularly useful for optoelectronics or flexible electronics[1,2] The electrical properties of graphene including work function, mobility, and sheet resistance are strongly affected by its interaction with surroundings,[3,4] which initiated the studies to engineer the electrical properties of graphene by various doping methods. For example, the graphene can be doped by atomic substitution,[5] molecular adsorption,[6] covalent functionalization,[7] and the use of dielectric substrates,[8] self-assembled monolayers,[9,10] or metallic nanoparticles[11]. However, the covalent functionalization is unfavorable due to the significant decrease in carrier mobility and conductivity in spite of its advantage in stability. Compared to the covalent doping, the non-covalent doping by chemical species is advantageous because of insignificant drop in carrier mobility. However, the non-covalent doping is usually weak or unstable for n-type doping by small molecules in particular.[12] This has been partially overcome by vapor-phase doping with ethylene amine molecules that show higher stability proportional to molecular weight.[13] However, the dependence of molecular structures on the actual doping effect is needed to be further investigated to maximize the chemical doping by the amine species.

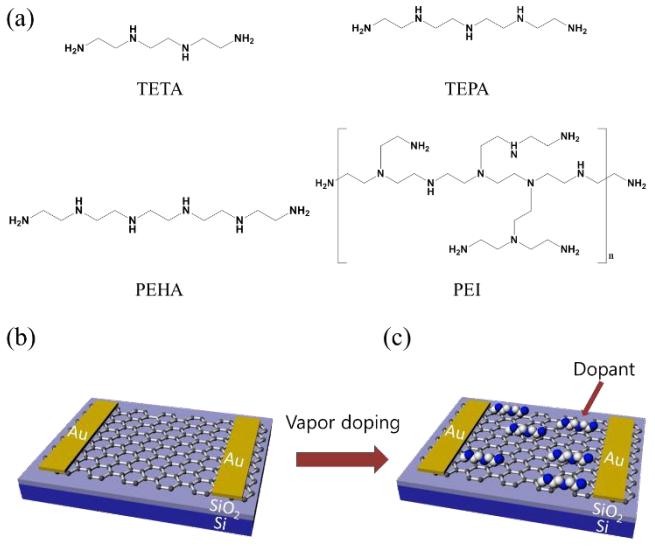

Fig. 1. (a) Chemical structures of the triethylene tetramine (TETA), tetraethylene pentamine (TEPA), pentaethylenehexamine (PEHA), and poly(ethyleneimine) (PEI). Schematic diagram of the vapor-phase doping process (b) before and (c) after.

Here, we selected a series of ethylene amines with different molecular weights and branched structures, including triethylene-tetramine (TETA), tetraethylenepentamine (TEPA), pentaethylene-hexamine (PEHA), and poly(ethyleneimine) (PEI) to measure the doping degree depending on molecular weight and structure. These molecules have 4, 5, 6 (linear), and n (branched) amino groups, respectively, and their molecular structures are shown in Fig. 1(a). Graphene samples used in this work were synthesized by low pressure chemical vapor deposition (LPCVD), following the literatures.[14,15] The graphene film grown on copper foil was covered by poly(methylmethacrylate) (PMMA) and floated in a 0.1 M ammonium persulfate ($(NH_2)_4S_2O_8$) aqueous solution. The PMMA supported graphene film was transferred to the 300 nm SiO_2/p^+Si substrate after all the copper layers were etched away and rinsed in deionized water. Then, graphene field-effect transistors (FETs) were

[a] Department of Chemistry, Seoul National University, Seoul 151-744, South Korea. E-mail: byunghee@snu.ac.kr
[b] Department of Physics & Astronomy, Seoul National University, Seoul 151-744, South Korea.
[c] Advanced Materials Team, Materials & Device Advanced Research Institute, LG Electronics, Seoul 137-724, South Korea

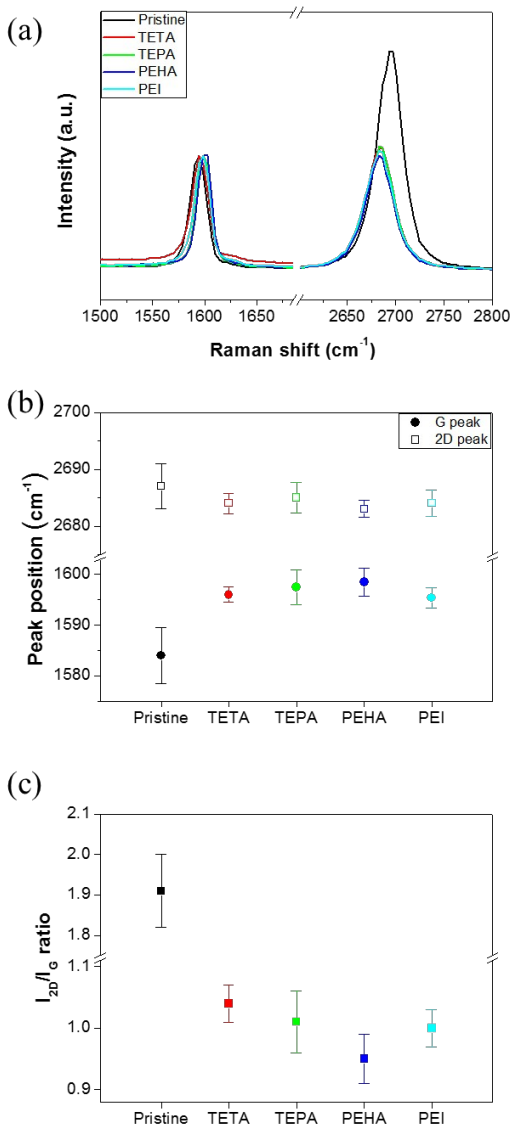

Fig. 2. Raman spectra of graphene doped with different ethylene amines and peak parameter analysis: (a) Raman spectra obtained from the pristine graphene and the doped graphene, (b) G and 2D peak positions for the pristine graphene and the doped graphene, (c) Statistical ratio I_{2D}/I_G for pristine graphene and doped graphene.

fabricated with Cr(5nm)/Au(30nm) source/drain electrodes to examine the electrical performance of doped graphene by different ethylene amines. Vapor-phase doping method reported in the literature was used.[13] The target substrate with each dopant droplet was placed in a glass dish (Fig. 1(b)) and baked at 120°C for vaporizing molecule on the surface of graphene during 30 min (Fig. 1(c)).

Raman spectroscopy was employed to investigate the properties of the ethylene amine-doped graphene (514 nm laser with 10 mW power).[16] Fig. 2(a) shows the Raman spectra of the monolayer graphene and of the doped graphene with various ethylene amines, in which the typical Raman peaks of graphene, the G band (1584 cm^{-1}) and the 2D band (2700 cm^{-1}), are observed.[17] The G peak position of graphene was blue-shifted from 1583.7 cm^{-1} to 1595.3 cm^{-1} (TETA), 1596.1 cm^{-1} (TEPA), 1596.9 cm^{-1} (PEHA), and 1595.7 cm^{-1} (PEI) due to the effect of the Fermi level shift on the phonon frequencies as a result of electron doping.[18] The red-shift of 2D peak position is also observed, which indicate the increasing electron concentrations (Fig. 2(b)). These results indicate that ethylene amine doping is stronger as the number of amino groups in the dopant increased (4, 5, and 6 for TETA, TEPA, and PEHA, respectively).[19,20] However, the PEI-doped graphene shows a lower doping degree although numerous amino groups in PEI molecule.

Noticeably, the I_{2D}/I_G ratio that is used to estimate the doping intensity decreased after ethylene amine vapor-phase doping. The intensity ratio of 2D to G peak (I_{2D}/I_G) is used to estimate the doping intensity that represented to decrease with doping.[21] The ratio was reduced from 1.93 for pristine graphene to 1.05, 1.02, 0.95, and 0.99 for TETA-, TEPA-, PEHA-, and PEI- doped graphene, respectively, shown in Fig. 2(c). Raman features that changing the peak positions and the I_{2D}/I_G ratio confirm the stronger n-doping of linear ethylene amines as the number of amino groups increases. Thus, the amount of electrons injection per covered area is expected to increase with the number of amino groups. However, PEI-doped graphene shows a weaker n-doping effect, even though it has more amino groups than linear molecules.

This implies that the doping concentration depends not only on the number of amine groups but also the branched structure of polymeric molecules. We suppose that the amine functional groups in PEI cannot be easily rearranged to maximize the interaction with graphene due to the steric confinement by long and branched structures. Therefore, the charges are inhomogeneously confined, and the carrier concentration is decreased, resulting in the Dirac point to shift back close to zero voltage.[22]

The electrical properties of a dozen of graphene transistors were measured to investigate the n-doping effects of the ethylene amine dopants (Agilent 2602). The graphene transistors were fabricated by CVD graphene films grown from a single batch to avoid inconsistencies in graphene devices and doping processes. Fig. 3(a) shows the current-voltage characteristics of the back-gated pristine and of n-doped graphene FETs. At first, the Dirac voltage of the pristine graphene transistors was measured to be at 18 ± 5 V. The Dirac voltages were shifted to -94 ± 7 V, -135 ± 6 V, -158 ± 8 V, and -58 ± 7 V for TETA-, TEPA-, PEHA-, and PEI-doped graphene, respectively. In addition, the carrier concentrations were calculated to be 7.1×10^{12} for TETA doped graphene, 9.2×10^{12} for TEPA doped graphene, 1.01×10^{13} for PEHA doped graphene, and 4.9×10^{12} cm^{-2} for PEI-doped graphene by utilizing Eq. (2):[1,21]

$$n = -\alpha(V_g - V_{CNP}) \quad (1)$$

where $\alpha = 7.2 \times 10^{10}$ cm^{-2} V^{-1} and V_{CNP} is the charge neutral point voltage. These findings are consistent with the results obtained from the Raman analysis, implying that the charge transfer between molecules and graphene is maximized by increasing the functional groups in the linear dopant. The mobility of each device was calculated in the linear regime, using the Eq. (2):[8,9]

$$I_D = \frac{WC_i}{L} V_D \mu (V_G - V_T) \quad (2)$$

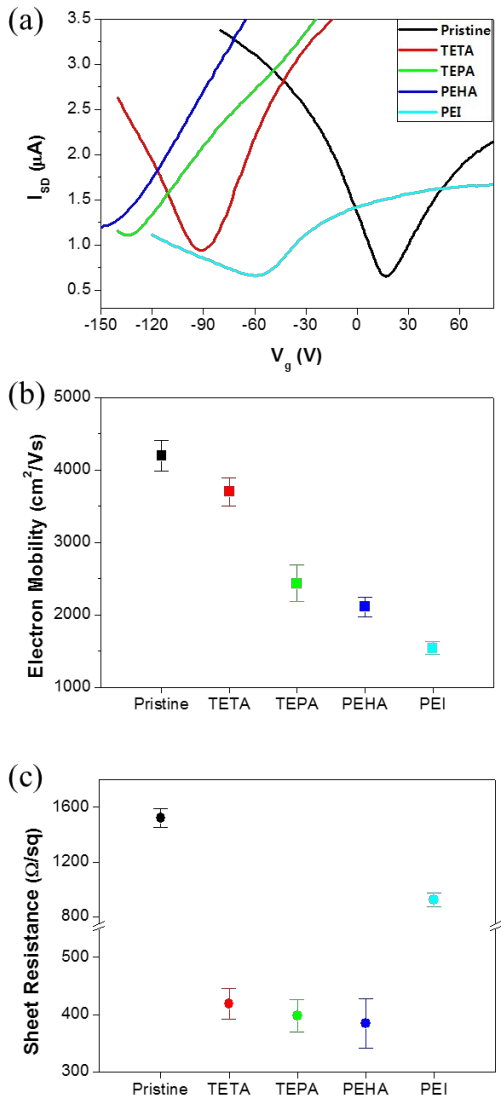

Fig. 3. (a) Current-voltage transfer characteristics, (b) electron mobility, and (c) sheet resistance of pristine (black), TETA-doped (red), TEPA-doped (green), PEHA-doped (blue), and PEI-doped (cyan) graphene FET devices.

where C_i = 1.08 × 10^{-8} F cm^{-2}, V_D = 0.01 V, W = 230 μm, and L = 180 μm. The estimated mobility of pristine graphene devices yields 4200 ± 210 cm^2 V^{-1} s^{-1} (hole region) and 4060 ± 178 cm^2 V^{-1} s^{-1} (electron region) that relatively high mobility for its scales. However, only the electron mobility of the doped graphene devices was compared, due to the lack of hole-region points. Doped graphene devices showed decreasing electron mobility as the number of amino groups increased. The electron mobility was measured to be 3700 ± 190, 2437 ± 250, 2110 ± 130, and 1540 ± 90 cm^2 V^{-1} s^{-1} for TETA-, TEPA-, PEHA-, and PEI-doped transistors, respectively. The results are plotted in Fig. 3(b). To further clarify this doping characteristics, the sheet resistance of pristine and of doped graphene were measured on SiO_2 (300 nm)/Si substrates (Fig. 3(c)) with 4-terminal measurement with Van der Pauw geometry. The sheet resistance of pristine graphene gradually decreased from 1520.0 ± 67.6 Ω sq^{-1} to 418.6 ± 26.6 Ω sq^{-1}, 397.6 ± 28.0 Ω sq^{-1}, and 385.0 ± 43.4 Ω sq^{-1} for

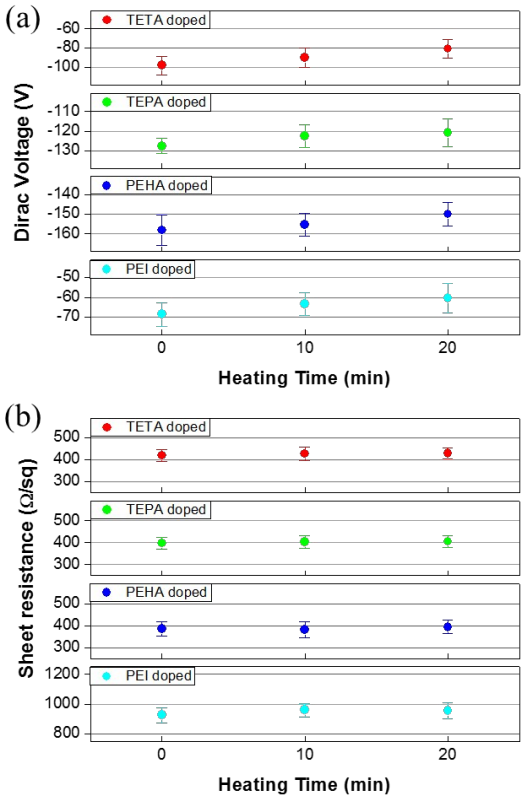

Fig. 4. Changes in (a) Dirac voltage and (b) sheet resistance of TETA-doped (red), TEPA-doped (green), PEHA-doped (blue), and PEI-doped (cyan) graphene FETs with increasing annealing time at 90°C.

TETA-, TEPA-, and PEHA-doped graphene, respectively. However, PEI-doped graphene showed a high sheet resistance of 925.4 ± 49.0 Ω sq^{-1}, as PEI induced a lower doping effect on graphene. The electrical measurement results show the degradation of the mobility and the sheet resistance in doped graphene due to the amino functional groups acted as charge impurities on graphene by the potential difference between pristine graphene and ethylene amines.[23]

The durability of doping is another issue in the fabrication of n-doped graphene devices. To compare the stability of doping for each dopant, the change of the Dirac voltage position and the sheet resistance with different ethylene amine doped graphene were all measured. Fig. 4 depicts the changes with respect to the heating time in ambient conditions. After the n-doped graphene devices were heated during 20 min at 90°C, the Dirac voltage was changed from -98.3 ± 8.3 V to -80.8 ± 9.7 V for TETA, from -127.5 ± 3.7 V to -120.8 ± 5.4 V for TEPA, from -157.4 ± 4.8 V to -151.8 ± 5.6 V for PEHA, and from -68.7 ± 5.1 V to -60.5 ± 4.5 V for PEI, respectively. In addition, the sheet resistance was shifted from 418.6 ± 26.6 Ω sq^{-1} to 429.5 ± 23.6 Ω sq^{-1} for TETA, from 397.6 ± 28.0 Ω sq^{-1} to 404.9 ± 26.4 Ω sq^{-1} for TEPA, from 385.0 ± 43.4 Ω sq^{-1} to 393.5 ± 30.6 Ω sq^{-1} for PEHA, and from 925.4 ± 49.0 Ω sq^{-1} to 956.7 ± 53.4 Ω sq^{-1} for PEI. Even after heating at 90 °C for 20 min, relatively stable Dirac voltage and sheet resistance were obtained, which is important for the practical use of the n-doped graphene for various device applications that require stable operation for a long period of time.

In summary, we have investigated the effect of the dopant structure as well as the number of amines group on the actual doping degree using optical and electrical analyses. It was expected that the carrier concentration increases with the number of amine groups and molecular weight. However, the PEI with branched ethylene amine structures showed the weak doping effect although it possesses the largest number of amino groups per molecule. We suppose that the polymeric amines tend to form a randomly oriented amorphous structure, possibly resulting in inhomogeneous coverage or inefficient charge transfer from amine groups to graphene. In contrast, non-polymeric molecules are readily self-assembled on graphene to form a regular structure,[24] which can maximize the charge transfer interaction for higher n-doping concentration. Thus, we conclude that not only the number of amine groups but also the non-polymeric structure with less steric confinement is an important factor to be considered in the development of stronger and more stable n-dopants.

Acknowledgements

B.H.H acknowledges financial support from the Basic Science Research Program (2012M3A7B4049807), the National Research Lab (NRL) Program(2011-0017587), and the Global Research Lab (GRL) Program(2011-0021972) through the National Research Foundation of Korea funded by the Ministry of Science, ICT & Future, Korea.

Notes and references

1 K. S. Novoselov, A. K. Geim, S. V. Morozov, D. Jiang, Y. Zhang, S. V. Dubonos, I. V. Grigorieva, and A. A. Firsov, *Science*, 2004, **306**, 666.
2 Y. Zhang, Y.-W. Tan, H. L. Stromer, and P. Kim, *Nature*, 2005, **438**, 201.
3 A. H. Castro Neto,, F. Guinea, N. M. R. Peres, K. S. Novoselov, and A. K. Geim, *Rev. Mod. Phys*., 2009, **81**, 109.
4 C. R. Dean, A. F. Young, I. Meric, C. Lee, L. Wang, S. Sorgenfrei, K. Watanabe, T. Taniguchi, P. Kim, Shepard, K. L. and J. Hone. *Nat. Nanotechnol*., 2010, **5**, 722.
5 D.C. Wei, Y.Q. Liu, Y. Wang, H.L. Zhang, L.P. Huang, G. Yu, *Nano Lett*., 2009, **9**, 1752.
6 S. Ryu, L, Liu, S. Berciaud, Y. J. Yu, H. Liu, P. Kim, G. W. Flynn, and L. E. Brus, *Nano Lett.*, 2010, **10**, 4944.
7 M. Seifert, J. E. B. Vargas, M. Bobinger, M. Sachsenhauser, A. W. Cummings, S. Roche and J. A. Garrido, *2D Mater*., 2015, **2**, 024008.
8 Z. Hu, D. P. Sinha, J. U. Lee and M. Liehr, *J. Appl, Phys*., 2014, **115**, 194507.
9 J. Park, W. H. Lee, S. Huh, S. H. Sim, S. B. Kim, K. Cho, B. H. Hong, and K. S. Kim, *J. Phys Chem. Lett*., 2011, 2, 841.
10 Y. Kim, J. Park, J. Kang, J. M. Yoo, K. Choi, E. S. Kim, J.-B. Choi, C. Hwang, K. S. Novoselov and B. H. Hong, *Nanoscale*, 2014, **6**, 9545.
11 K. Pi, K. M. McCreary, W. Bao, Wei Han, Y. F. Chiang, Yan Li, S.-W. Tsai, C. N. Lau, and R. K. Kawakami, *Phys. Rev. B*, 2009, **80**, 075406.
12 S. Some, J. Kim, K. Lee, A. Kulkarni, Y. Yoon, S. Lee, T. Kim, and H. Lee, *Adv. Mater*., 2012, **24**, 5481.
13 Y. Kim, J. Ryu, M. Park, E. S. Kim, J. M. Yoo, J. Park, J. H. Kang and B. H. Hong, *ACS Nano,* 2014, **8**, 868.
14 X. Li, W. Cai, J. An, S. Kim, J. Nah, D. Yang, R. Piner, A. Velamakanni, I. Jung, E. Tutuc, S. K. Banerjee, L. Colombo, and R. S. Ruoff, *Science,* 2009, **324**, 1312.
15 S. Bae, H. Kim, Y. Lee, X. Xu, J.-S. Park, Y. Zheng, J. Balakrishnan, T. Lei, H. R. Kim, Y. I. Song, Y.-J. Kim, K. S. Kim, B. Ozyilmaz, J.-H. Ahn, B. H. Hong, and S. Iijima, *Nat. Nanotechnol*., 2010, **5**, 574.
16 A. C. Ferrari, D. M. Basko, *Nat. Nanotechnol*., 2013, **8**, 235.
17 A. C. Ferrari, J. C. Meyer, V. Scardaci, C. Casiraghi, M. Lazzeri, F. Mauri, S. Piscanec, D. Jiang, K. S. Novoselov, S. Roth, and A. K. Geim, *Phys. Rev. Lett*., 2006, **97**, 187401.
18 A. Das, S. Pisana, B. Chakraborty, S. Piscanec, S. K. Saha, U. V. Waghmare, K. S. Novoselov, H. R. Krishnamurthy, A. K. Geim, A. C. Ferrari and A. K. Sood, *Nat. Nanotechnol*., 2008, **3**, 210.
19 A. K. Geim and K. S. Novoselov, *Nat. Mater*., 2007, **6**, 183.
20 T. Mohiuddin, A. Lombardo, R. Nair, A. Bonetti, G. Savini, R. Jalil, N. Bonini, D. Basko, C. Galiotis, N. Marzari, K. Novoselov, A. Geim, and A. Ferrari, *Phys. Rev. B,* 2009, **79**, 205433.
21 C. Casiraghi, S. Pisana1, K. S. Novoselov, A. K. Geim and A. C. Ferrari, *Appl. Phys. Lett*., 2007, **91**, 233108.
22 K. M. McCreary, K. Pi, A. G. Swartz, W. Han, W. Bao, C. N. Lau, F. Guinea, M. I. Katsnelson, and R. K. Kawakami, *Phys. Rev. B*, 2010, **81**, 115453
23 A. Deshpande, C. H. Sham, J. M. P. Alaboson, J. M. Mullin, G. C. Schatz, and M. C. Hersam, *J. Am. Chem. Soc*., 2012, **134**, 16759.
24 W. H. Lee, J. Park, S.H. Sim, S. Lim, K. S. Kim, B. H. Hong, K. Cho, *J. Am. Chem. Soc*., 2011, **133**, 4447